
Water and urea interactions with the native and unfolded forms of a β -barrel protein

KRISTOFER MODIG,¹ ELIZABETH KURIAN,^{2,3} FRANKLYN G. PRENDERGAST,² AND BERTIL HALLE¹

¹Department of Biophysical Chemistry, Lund University, SE-22100 Lund, Sweden

²Department of Biochemistry and Molecular Biology, Mayo Foundation, Rochester, Minnesota 55905, USA

(RECEIVED June 15, 2003; FINAL REVISION August 20, 2003; ACCEPTED August 20, 2003)

Abstract

A fundamental understanding of protein stability and the mechanism of denaturant action must ultimately rest on detailed knowledge about the structure, solvation, and energetics of the denatured state. Here, we use ¹⁷O and ²H magnetic relaxation dispersion (MRD) to study urea-induced denaturation of intestinal fatty acid-binding protein (I-FABP). MRD is among the few methods that can provide molecular-level information about protein solvation in native as well as denatured states, and it is used here to simultaneously monitor the interactions of urea and water with the unfolding protein. Whereas CD shows an apparently two-state transition, MRD reveals a more complex process involving at least two intermediates. At least one water molecule binds persistently (with residence time >10 nsec) to the protein even in 7.5 M urea, where the large internal binding cavity is disrupted and CD indicates a fully denatured protein. This may be the water molecule buried near the small hydrophobic folding core at the D–E turn in the native protein. The MRD data also provide insights about transient (residence time <1 nsec) interactions of urea and water with the native and denatured protein. In the denatured state, both water and urea rotation is much more retarded than for a fully solvated polypeptide. The MRD results support a picture of the denatured state where solvent penetrates relatively compact clusters of polypeptide segments.

Keywords: Protein denaturation; fatty acid-binding protein; urea; solvent exchange; magnetic relaxation dispersion

Despite the widespread use of urea in studies of protein stability and folding thermodynamics (Kauzmann 1959; Tanford 1970; Myers et al. 1995), the molecular mechanism whereby urea unfolds proteins has not been established. Solvent denaturation is a result of altered protein–solvent interactions, but it is not clear whether denaturants like urea act directly by binding to the protein surface or indirectly by perturbing solvent-mediated hydrophobic interactions or by

a combination of these mechanisms. The direct mechanism is made plausible by the structural similarity between urea and the peptide group, suggesting that urea–peptide interactions, like peptide–peptide interactions, can compete favorably with water–peptide interactions. If this is the case, then solvent denaturation can be driven simply by the exposure of more binding sites in the denatured protein (Schellman 1987). The indirect mechanism is supported by the observation that urea enhances the solubility of not-too-small nonpolar solutes or groups (Wetlaufer et al. 1964; Shimizu and Chan 2002) and, by implication, weakens the hydrophobic stabilization of the folded protein.

A fundamental understanding of protein stability, including the mode of denaturant action, must be based on experimental characterization of the structure, solvation, and energetics of the denatured state at the level of detail that has been achieved for the native state (Dill and Shortle

Reprint requests to: Bertil Halle, Department of Biophysical Chemistry, Lund University, Box 124, SE-22100 Lund, Sweden; e-mail: bertil.halle@bpc.lu.se; fax: 46-46-222-4543.

³Deceased.

Abbreviations: CD, circular dichroism; I-FABP, intestinal fatty acid-binding protein; MRD, magnetic relaxation dispersion; NOE, nuclear Overhauser effect.

Article and publication are at <http://www.proteinscience.org/cgi/doi/10.1110/ps.03262603>.

1991; Shortle 1996a). Denatured proteins have traditionally been modeled as fully solvated random coils, but a growing body of experimental evidence is challenging this view (Shortle 1996a; Denisov et al. 1999; Shortle and Ackerman 2001; Choy et al. 2002; Klein-Seetharaman et al. 2002). To quantitatively account for the often marginal stability of native proteins under physiological conditions, we need to examine denatured states from different vantage points using a variety of techniques. Although important progress has been made using NMR (Shortle 1996b) and small-angle scattering (Millet et al. 2002), few methods are available for directly probing the solvation of denatured proteins. One of these, water ^{17}O magnetic relaxation dispersion (MRD), has previously been used to monitor both internal and surface hydration during thermal denaturation (Denisov and Halle 1998) and solvent denaturation by guanidinium chloride (Denisov et al. 1999). Here, we use ^{17}O and ^2H MRD to examine hydration as well as denaturant interactions during the urea-induced unfolding of the apo form of intestinal fatty acid-binding protein (I-FABP). ^2H MRD has previously been used to study DMSO-protein interactions (Jóhannesson et al. 1997), but this is the first MRD study to monitor solvent and cosolvent/denaturant simultaneously.

Like the other members of the family of lipid-binding proteins (Banaszak et al. 1994; Zimmerman and Veerkamp 2002), the 15-kD cytoplasmic protein I-FABP has a β -clam structure composed of 10 antiparallel strands that enclose a very large (500–1000 \AA^3) internal binding cavity (see Fig. 1). Lipids are thought to enter the cavity via a small “portal” lined by two short α -helices. The folding thermodynamics and kinetics of I-FABP have been studied extensively (Ropson et al. 1990; Ropson and Frieden 1992; Clark et al. 1997,

1998; Kim et al. 1997; Ropson and Dalessio 1997; Burns et al. 1998; Dalessio and Ropson 1998, 2000; Kim and Frieden 1998; Hodsdon and Frieden 2001; Yeh et al. 2001; Chattopadhyay et al. 2002a,b; Nikiforovich and Frieden 2002). The equilibrium denaturation of I-FABP by urea appears to be two-state and cooperative when monitored by optical spectroscopy, but NMR studies have indicated intermediate states (Ropson and Frieden 1992; Hodsdon and Frieden 2001).

Although the folding of β -sheet proteins does not appear to differ fundamentally from that of proteins with a classical hydrophobic core (Capaldi and Radford 1998), it is of interest to examine the role of the solvent-filled cavity in solvent denaturation. Another reason for choosing I-FABP for this denaturation study is that its internal and external hydration has been characterized in detail by ^{17}O and ^2H MRD (Wiesner et al. 1999; Modig et al. 2003). Briefly, these MRD studies have shown that the 20–25 water molecules that occupy the binding cavity (Scapin et al. 1992) remain trapped for more than 10 nsec before exchanging with external solvent. While residing in the cavity, these water molecules exchange among internal hydration sites on a time scale of 1 nsec. This intracavity exchange has also been characterized by molecular simulations (Likic and Prendergast 2001; Bakowies and van Gunsteren 2002). In addition, a singly buried water molecule (labeled W135 in the I-FABP crystal structure) is buried near a hydrophobic cluster at the turn between β -strands D and E (see Fig. 1). This water molecule is conserved across the family of lipid-binding proteins, and must therefore contribute importantly to the stability of the native protein structure (Likic et al. 2000). W135 has a long residence time (Likic et al. 2000; Likic and Prendergast 2001; Bakowies and van Gunsteren 2002), and is thought to be the main (possibly, the only) contributor to the low-field ^{17}O dispersion (Wiesner et al. 1999; Modig et al. 2003). Because the hydrophobic cluster at the D–E turn forms early on the folding pathway (Ropson and Frieden 1992; Kim et al. 1997; Hodsdon and Frieden 2001; Yeh et al. 2001; Chattopadhyay et al. 2002b; Nikiforovich and Frieden 2002), we can use W135 as an MRD marker for this (un)folding event.

An important aspect of the present work is the separation of water and urea contributions to the observed ^2H relaxation. This allows us to directly probe urea interactions with I-FABP across the unfolding transition, while also monitoring the competing water interactions. The available structural data on urea-protein interactions are limited and, with few exceptions (Dötsch et al. 1995; Dötsch 1996), are restricted to native proteins (Lumb and Dobson 1992; Liepinsh and Otting 1994; Pike and Acharya 1994). Computer simulations of proteins in molecular solvent are still a long way from being able to access the time scales on which solvent-induced protein unfolding takes place. Therefore, simulations have so far only provided information about

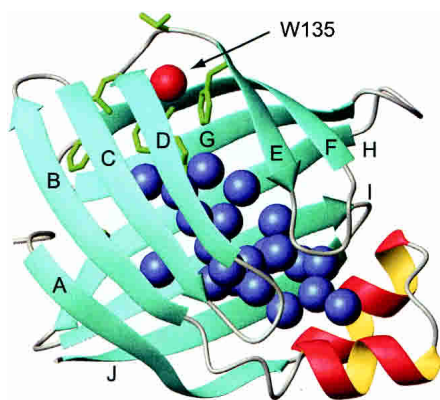


Figure 1. Crystal structure of apo I-FABP from PDB entry 1IFC (Scapin et al. 1992) with the 10 β -strands labeled. Water oxygens in the large binding cavity are colored blue, and the singly buried water oxygen in the D–E turn (labeled W135 in 1IFC) is red. Some of the hydrophobic residues thought to be involved in the hydrophobic folding core are colored green: from *bottom* to *top*, Ile40 (barely visible behind strand B), Phe47, Phe62, Trp82, Leu64, Phe68, and Val66. The figure was generated with the program MOLMOL (Koradi et al. 1996).

urea–protein interactions in the native state or in partially unfolded states at very high temperatures (Tirado-Rives et al. 1997; Cafilisch and Karplus 1999).

Results and Discussion

Water ^{17}O relaxation in bulk aqueous urea solutions

For reference purposes, we measured the water ^{17}O relaxation rate in protein-free samples with the same solvent composition as in the I-FABP solutions. The ^{17}O relaxation rate R_{bulk} in these bulk urea solutions increases with the urea concentration C_{U} (in mol dm $^{-3}$) as

$$R_{\text{bulk}}/R_{\text{bulk}}^0 = 1 + 5.70 \times 10^{-3} C_{\text{U}} + 1.16 \times 10^{-3} C_{\text{U}}^2 + 1.04 \times 10^{-5} C_{\text{U}}^3 \quad (1)$$

In Figure 2, this weak concentration dependence is contrasted with the five to six times stronger urea-induced viscosity enhancement (Kawahara and Tanford 1966). The insensitivity of the water ^{17}O (Bagno et al. 1993) and ^2H (Yoshida et al. 1998) relaxation rates to the presence of urea has been noted previously. In fact, at the low urea concentrations ($C_{\text{U}} < 2$ M) investigated previously, the effect of urea was barely significant.

Assuming that only the n_{S} water molecules in the first hydration shell of urea differ from bulk water, we can express the coefficient of the linear term in equation 1 as $V_{\text{W}}^0 n_{\text{S}} (\tau_{\text{S}}/\tau_{\text{bulk}} - 1)$, where τ_{S} and τ_{bulk} are the rotational correlation times of water molecules in the hydration shell and in bulk water, respectively, and $V_{\text{W}}^0 = 1.80 \times 10^{-2}$ dm 3 mole $^{-1}$ is the molar volume of water. Taking $n_{\text{S}} = 12.6$, as

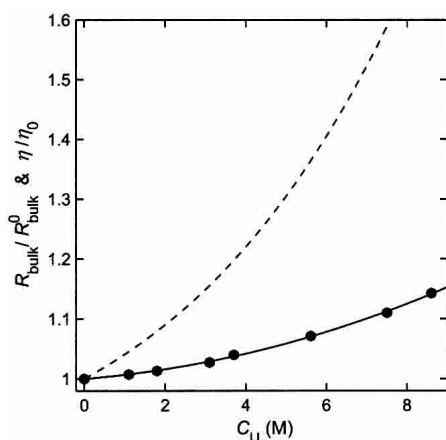


Figure 2. Relative variation of the water ^{17}O relaxation rate R_{bulk} and shear viscosity η with urea concentration in aqueous solutions at 27°C. The R_{bulk} data (filled circles) were fitted to the cubic polynomial in equation 1 (solid curve). The viscosity (dashed curve) is described by the empirical relation $\eta/\eta_0 = 1 + 3.75 \times 10^{-2} C_{\text{U}} + 3.15 \times 10^{-3} C_{\text{U}}^2 + 3.10 \times 10^{-4} C_{\text{U}}^3$ (Kawahara and Tanford 1966).

obtained by integrating the first peak in simulated pair correlation functions (Kuharski and Rossky 1984), we find that the rotation of water molecules in contact with urea is retarded by merely 3% ($\tau_{\text{S}}/\tau_{\text{bulk}} = 1.025$). Concerning rotational dynamics, water in urea solutions can therefore be regarded as essentially unperturbed bulk water. This conclusion is consistent with the nearly ideal thermodynamic behavior of aqueous urea solutions (Ellerton and Dunlop 1966) and the finding, in several molecular simulation studies (Kuharski and Rossky 1984; Åstrand et al. 1994; Vanzi et al. 1998; Kallies 2002), that the intermolecular structure of water is virtually unaffected by urea. Simulations also show that the retardation of water rotation in the urea hydration shell is small, for example, 6% in one study (Åstrand et al. 1994).

The curvature in equation 1 may be attributed either to overlap of hydration regions, which then would have to extend beyond the first shell ($n_{\text{S}} = 12.6$ corresponds to $C_{\text{U}} = 3.7$ M), or to urea self-association. Molecular simulation studies have provided conflicting results on urea self-association, presumably due to force-field imperfections (Sokolic et al. 2002).

The negligibly small perturbation of water rotational dynamics by urea may be contrasted with that of other small nonelectrolyte solutes (Bagno et al. 1993). Thus, the quantity $n_{\text{S}}(\tau_{\text{S}}/\tau_{\text{bulk}} - 1)$ is in the range 5–8 for methanol, ethylene glycol, and DMSO, while we obtain 0.32 for urea. This order-of-magnitude difference can be attributed to the dynamic retardation factor ($\tau_{\text{S}}/\tau_{\text{bulk}} - 1$), because the number n_{S} of water molecules in the hydration shell should vary by less than a factor 2 among these solutes. For proteins, MRD data yield the average of ($\tau_{\text{S}}/\tau_{\text{bulk}} - 1$) over the heterogeneous surface; typically, this average is in the range 4–5 (Denisov et al. 1996; Halle 1998).

Solvent ^{17}O and ^2H relaxation dispersion in I-FABP solutions

The water ^{17}O magnetic relaxation dispersion (MRD) profile $R_1(\omega_0)$ exclusively monitors the dynamics of water molecules in association with the protein, whereas the ^2H MRD profile also contains a pH-dependent contribution from labile hydrogens in the protein that exchange rapidly with the solvent (Denisov and Halle 1995; Halle et al. 1999; Halle and Denisov 2001). In the case of native I-FABP at pH 7, the labile hydrogen contribution appears to be insignificant (Wiesner et al. 1999).

When the solvent contains urea and D_2O , hydrogen exchange distributes the ^2H nuclei uniformly among water and urea molecules. The ^2H magnetization therefore reports on both species. Separate water and urea resonance peaks are observed only at high magnetic fields, where water–urea hydrogen exchange is slow on the chemical shift time scale. Nevertheless, because the exchange remains in the slow to

intermediate regime on the relaxation time scale, the individual water and urea ^2H relaxation rates can be determined also at low fields from a quantitative analysis of the bi-exponential ^2H magnetization recovery (see Materials and Methods).

For most proteins, the water ^{17}O and ^2H MRD profiles can be described by a constant term (denoted α) plus a single Lorentzian dispersion (β term) with a correlation time τ_β that matches the rotational correlation time τ_R of the protein, which is 7 nsec for I-FABP in water with 50% deuterium at 27°C (Wiesner et al. 1999). For I-FABP and other lipid-binding proteins, the 20–25 water molecules occupying the large internal binding cavity exchange among hydration sites within the cavity on a time scale of 1 nsec (Wiesner et al. 1999; Modig et al. 2003), thus giving rise to a high-frequency dispersion (γ term). Because of the short correlation time ($\tau_\gamma \approx 1$ nsec), only the low-frequency flank of the γ dispersion can be accessed by ^{17}O or ^2H MRD. In summary, the MRD profile for native I-FABP is described by a constant plus two dispersive terms (see equation 6). The five parameters that define this dispersion profile can be rigorously transformed into well-defined molecular parameters (see Materials and Methods).

Internal hydration of I-FABP during denaturation by urea

^{17}O and ^2H MRD profiles were measured in apo I-FABP solutions at pH 7, 27°C, and 10 different urea concentrations from 0 to 8.6 M (see Table 1). We shall first discuss the ^{17}O data, which only report on water molecules. The full data set is shown in Figure 3. To reduce the number of adjustable parameters, we omit the highest-frequency point in each dispersion profile. This allows us to describe the relaxation data in terms of a single Lorentzian dispersion, $\beta\tau_\beta(1 + [\omega_0\tau_\beta]^2)^{-1}$, and a renormalized constant $\tilde{\alpha} = \alpha + \gamma\tau_\gamma$ (see Materials and Methods). The β parameter can be transformed into $N_I^W S_{I,W}^2 + N_C^W S_{C,W}^2 A_{C,W}^2$ (see equation 7b). We denote this reduced quantity by β_{red}^W and refer to it as the

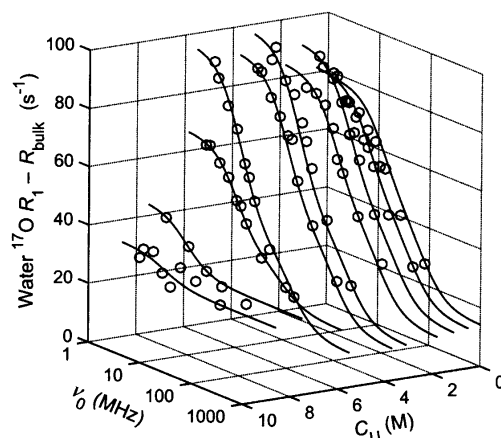


Figure 3. Water ^{17}O MRD profiles at 27°C in aqueous solutions of apo I-FABP at pH 7.0 with 0–8.6 M urea. The vertical axis measures the excess ^{17}O relaxation rate, $R_1 - R_{\text{bulk}}$, normalized to $N_T^W = 22,600$ ($C_P = 2.38$ mM) to remove the effect of slight variations in protein concentration. The curves were obtained from a global fit of all data points to a three-state model (with some of the parameters fixed at plausible values), but is mainly intended as a visual guide.

internal hydration parameter. N_I^W and N_C^W are the numbers of long-lived (residence time >10 nsec) water molecules in singly occupied cavities and in the large binding cavity, respectively, and the other variables are orientational order parameters with a maximum value of 1 (see Materials and Methods).

For native I-FABP in the absence of urea, the single-Lorentzian fit yields $\beta_{\text{red}}^W = 2.4 \pm 0.3$, in agreement with a previous MRD study (Wiesner et al. 1999). On the basis of an analysis of the 1.2 Å crystal structure of apo I-FABP (Scapin et al. 1992), this internal hydration parameter can be attributed to $N_I^W = 1$ singly buried water molecule (W135 in the D–E turn) and $N_C^W = 20$ –25 water molecules trapped in the large binding cavity (see Fig. 1). The single-Lorentzian fit also yields a correlation time $\tau_\beta = 6.8 \pm 0.5$ nsec for native I-FABP. This agrees with the rotational correlation time of native I-FABP, $\tau_R = 7.2$ nsec determined by ^{15}N NMR relaxation (Hodsdon and Cistola 1997) and fluorescence depolarization (Frolov and Schroeder 1997) and scaled to the viscosity (0.968 cP) of our isotope-enriched water.

Figure 4 shows the variation of the internal hydration parameter β_{red}^W with the urea concentration C_U along with the far-UV CD denaturation profile, converted to the apparent fraction f of native protein (Santoro and Bolen 1998). The hydration parameter β_{red}^W and the combined CD data (at 216 and 222 nm) were analyzed in terms of a two-state denaturation equilibrium $N \leftrightarrow D$ with a denaturation free energy linear in C_U (see Materials and Methods). The resulting parameters $C_{1/2}$ and m are given in Table 2. Our CD parameters fall within the rather wide range reported from previous CD and fluorescence studies (Ropson et al. 1990;

Table 1. Composition of MRD samples

| Sample no. | C_U (M) | x_U | C_P (mM) | $N_T^W \times 10^{-3}$ | $N_T^U \times 10^{-3}$ |
|------------|-----------|-------|------------|------------------------|------------------------|
| 1 | 0 | 0 | 2.38 | 22.6 | 0 |
| 1 | 0.5 | 0.009 | 2.38 | 22.6 | 0.20 |
| 1 | 1.1 | 0.020 | 2.38 | 22.6 | 0.47 |
| 3 | 1.8 | 0.034 | 2.28 | 23.7 | 0.84 |
| 1 | 3.1 | 0.061 | 2.38 | 22.6 | 1.47 |
| 3 | 3.7 | 0.074 | 2.28 | 23.7 | 1.90 |
| 1 | 5.5 | 0.117 | 2.38 | 22.6 | 2.99 |
| 2 | 5.8 | 0.125 | 2.30 | 23.4 | 3.36 |
| 2 | 7.5 | 0.170 | 2.30 | 23.4 | 4.80 |
| 3 | 8.6 | 0.203 | 2.28 | 23.7 | 6.02 |

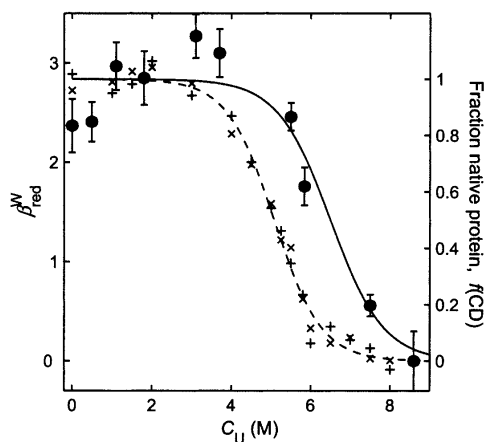


Figure 4. Variation of the internal hydration parameter $\beta_{\text{red}}^{\text{W}}$ (filled circles) during urea-denaturation of 2.3 mM apo I-FABP at pH 7.0 and 27°C. $\beta_{\text{red}}^{\text{W}}$ was derived from single-Lorentzian fits to ^{17}O MRD profiles. The ellipticity at 216 nm (+) and 222 nm (×) was measured on 11.5 μM apo I-FABP solutions at 27°C, and is displayed as the apparent native fraction f . The curves resulted from fits according to the standard two-state linear free energy model.

Burns et al. 1998; Dalessio and Ropson 1998, 2000), but do not agree quantitatively with any one of them. Apparently, the salt (and buffer) concentration has a significant effect on the denaturation equilibrium (see Table 2).

In line with previous reports, our CD data are well described by a two-state model. When probed by the internal hydration parameter $\beta_{\text{red}}^{\text{W}}$, however, denaturation is seen to require significantly higher urea concentration: $C_{1/2} = 6.5$ M versus 5.1 M from CD. Moreover, the $\beta_{\text{red}}^{\text{W}}$ data are not well described by a two-state model if $\beta_{\text{red}}^{\text{W}}(\text{N})$ is taken to be independent of C_{U} (as was done in the fit of Fig. 4). Specifically, $\beta_{\text{red}}^{\text{W}}$ increases by nearly one unit in the range 0–3 M urea, where the CD data indicate that the protein is fully native. For native apo I-FABP, $\beta_{\text{red}}^{\text{W}}$ is thought to have roughly equal contributions from one singly buried water molecule and 20–25 water molecules in the binding cavity (Modig et al. 2003). The vanishing of $\beta_{\text{red}}^{\text{W}}$ at 8.6 M urea (see Fig. 4) therefore indicates that the binding cavity has vanished (or, at least, has opened up sufficiently to allow subnanosecond water exchange with the bulk solvent) and that the hydrophobic cluster at the D–E turn has disintegrated (or, at least, has only a transient existence). Our data show that this unfolding takes place at a higher urea concentration than the secondary structure changes probed by CD. Because α -helices contribute twice as much as β -strands to the specific ellipticity in the far-UV range (Kelly and Price 1997), the CD data are expected to overemphasize the two short α -helices (see Fig. 1), which may unfold at lower urea concentration than the cooperatively stabilized β -barrel.

The increase of $\beta_{\text{red}}^{\text{W}}$ below 3 M urea may reflect an equilibrium folding intermediate, but could also result from trapping of one or two previously short-lived water mol-

ecules by urea molecules in long-lived association with I-FABP. The former explanation is supported by a ^1H - ^{15}N HSQC NMR study that revealed an intermediate protein structure with maximum population in the range 2.0–3.5 M urea (Hodsdon and Frieden 2001). That study also demonstrated that native-like structural elements persist up to 6.5 M urea, where CD and fluorescence data suggest that the protein is fully denatured. Also, this observation is consistent with our $\beta_{\text{red}}^{\text{W}}$ data, which exhibit a denaturation midpoint at 6.5 M. The observation of a substantial ^{17}O dispersion at such high urea concentrations implies that the residual structure is sufficiently permanent to trap water molecules for periods longer than 10 nsec. This residual structure may be related to the equilibrium folding intermediate detected at high urea concentrations (4–7 M) by ^{19}F NMR on fluorinated Trp82 (Ropson and Frieden 1992), the backbone NH of which donates a hydrogen bond to the long-lived internal water molecule (W135) in the D–E turn.

The correlation time τ_{β} obtained from the ^{17}O dispersion can be identified with the tumbling time τ_{R} of the protein. Unlike R_{bulk} (see Fig. 2), τ_{β} should therefore be proportional to the solvent viscosity; that is, a hydrodynamic continuum description should apply. To remove the trivial dependence of τ_{β} on the urea concentration C_{U} via the viscosity η (Kawahara and Tanford 1966), we multiply τ_{β} by $\eta(0)/\eta(C_{\text{U}})$. For a rigid globular protein, τ_{R} is proportional to the hydrodynamic volume. The viscosity-corrected τ_{β} should therefore reflect any global changes in protein structure during denaturation. As seen from Figure 5A, the viscosity-corrected τ_{β} hardly varies with urea concentration. This finding is not unexpected. The disappearance of the ^{17}O dispersion at 8.6 M urea (see Fig. 4) shows that there are no long-lived water molecules in the fully denatured protein; hence, $\beta(\text{D}) = 0$. The frequency-dependent part of R_1 is thus entirely due to the native protein fraction f (see equation 10). However, this argument is only valid for two-state denaturation. The invariance of τ_{β} in Figure 5A therefore tells us that the hydrodynamic volume of the intermediate species indicated by the C_{U} variation of the internal hydration parameter $\beta_{\text{red}}^{\text{W}}$ does not differ markedly from that of the native state. Moreover, it shows that the overall structure of the native state is essentially independent of urea concentration. This finding is consistent with previous studies showing that the native structures of BPTI (Liepinsh and Otting 1994) and hen lysozyme (Lumb and Dobson 1992; Pike and Acharya 1994) are essentially unaltered at high urea concentrations.

Surface hydration of I-FABP during denaturation by urea

The third piece of information obtained from the ^{17}O dispersion is the renormalized parameter $\tilde{\alpha} = \alpha + \gamma \tau_{\gamma}$, which can be transformed into $N_{\text{S}}^{\text{W}} \rho_{\text{S}}^{\text{W}} + N_{\text{C}}^{\text{W}} S_{\text{C,W}}^2 (1 - A_{\text{C,W}}^2) \omega_{\text{Q}}^2 \tau_{\gamma}$

Table 2. Results of two-state analysis of I-FABP denaturation curves

| $C_{1/2}$ (M) | m (kJ mole ⁻¹ M ⁻¹) | $C_p I$ (mM)/pH/T (°C) ^a | Method ^b | Reference ^c |
|---------------|---|-------------------------------------|---------------------|------------------------|
| 6.5 ± 0.1 | 3.7 ± 0.5 | 2.3 mM/10/7.0/27 | MRD | 1 |
| 5.1 ± 0.1 | 4.2 ± 0.4 | 11.5 μM/10/7.0/27 | CD | 1 |
| 4.10 ± 0.04 | 4.4 ± 0.3 | 6.6 μM/100/7.0/25 | CD | 2 |
| 4.24 ± 0.03 | 4.7 ± 0.3 | 6.6 μM/100/7.0/25 | F | 2 |
| 4.12 ± 0.03 | 4.8 ± 0.3 | 7 μM/100/8.0/25 | CD | 3 |
| 4.20 ± 0.04 | 5.1 ± 0.3 | 0.7 μM/100/8.0/25 | F | 3 |
| 5.43 | 7.4 ± 1.4 | 6–35 μM/20/7.2/20 | CD | 4 |
| 5.50 | 7.6 ± 0.2 | 1–7 μM/20/7.2/20 | F | 4 |
| 4.68 | — | —/20/6.6/25 | F | 5 |

^a C_p = protein concentration; I = ionic strength (including buffer).

^b MRD refers to $\beta_{\text{red}}^{\text{W}}$ (¹⁷O), CD to ellipticity near 220 nm, and F to fluorescence intensity near 340 nm.

^c References: (1) this work; (2) Dalessio and Ropson 1998; (3) Burns et al. 1998; (4) Ropson et al. 1990; (5) Hodsdon and Frieden 2001.

R_{bulk} (see equations 7a,c). We denote this reduced quantity by $\tilde{\alpha}_{\text{red}}^{\text{W}}$ and refer to it as the (apparent) surface hydration parameter. In the first term, N_S^{W} denotes the number of water molecules in contact with the external protein surface, estimated to 460 for native I-FABP (see Materials and Methods). The dynamic retardation factor $\rho_S^{\text{W}} = \tau_S/\tau_{\text{bulk}} - 1$ measures the relative slowing down of rotational diffusion for these water molecules. For native proteins, $\rho_S^{\text{W}} = 4-5$ (Denisov and Halle 1995; Halle 1998). For native I-FABP, the surface hydration contribution to $\tilde{\alpha}_{\text{red}}^{\text{W}}$ should therefore be close to $N_S^{\text{W}} \rho_S^{\text{W}} = 460 \times 4.5 = 2.1 \times 10^3$.

For native I-FABP in the absence of urea, the ¹⁷O dispersion yields $\tilde{\alpha}_{\text{red}}^{\text{W}} = (4.8 \pm 0.3) \times 10^3$. The contribution to $\tilde{\alpha}_{\text{red}}^{\text{W}}$ from the water molecules trapped in the ligand-binding cavity (the second term in $\tilde{\alpha}_{\text{red}}^{\text{W}}$) is therefore comparable to the surface water contribution. The quadrupole frequency

ω_Q and bulk relaxation rate R_{bulk} are known (see Materials and Methods and Fig. 2) and the correlation time for water exchange among hydration sites inside the cavity is $\tau_\gamma = 1.1 \pm 0.1$ nsec for native I-FABP (Wiesner et al. 1999; Modig et al. 2003). Combining all this, we obtain $N_C^{\text{W}} S_{C,W}^2 (1 - A_{C,W}^2) = 6.4 \pm 0.9$ for native I-FABP, in agreement with previous MRD studies (Wiesner et al. 1999; Modig et al. 2003).

One might expect $\tilde{\alpha}_{\text{red}}^{\text{W}}$ to increase with urea concentration as denaturation leads to enhanced solvent exposure (and, hence, larger N_S^{W}). In contrast, Figure 5B shows that $\tilde{\alpha}_{\text{red}}^{\text{W}}$ decreases monotonically across the denaturation transition. This behavior can be understood by recognizing that three different processes contribute to the C_U dependence of $\tilde{\alpha}_{\text{red}}^{\text{W}}$. Two of these processes are directly linked to the N ↔ D equilibrium. Denaturation greatly increases the solvent-accessible surface area A_S (see below), leading to a corresponding increase of the surface contribution to $\tilde{\alpha}_{\text{red}}^{\text{W}}$. But denaturation also disrupts the binding cavity, thereby eliminating the second contribution to $\tilde{\alpha}_{\text{red}}^{\text{W}}$. These two effects are large, but tend to cancel out.

The third process is the competition of water and urea molecules for surface sites, causing the number of water molecules per unit surface area to decrease with C_U . This competition can be taken into account by writing $N_S^{\text{W}} = N_W (1 - \theta)$, where N_W is the number of external hydration sites on the protein (proportional to A_S) and θ is the fraction of the surface occupied by bound urea molecules. According to the solvent exchange model (Schellman 1990, 1994), θ can be expressed in terms of the mean urea-binding constant K_U and the known urea and water activities (see Materials and Methods).

For proteins without large internal cavities, solvent denaturation only involves increase of surface area and solvent competition while thermal denaturation only involves the surface area effect. In such cases, the N → D transition is clearly reflected in $\tilde{\alpha}_{\text{red}}^{\text{W}}$ (Denisov and Halle 1998; Denisov et al. 1999). For I-FABP, the near cancellation of the

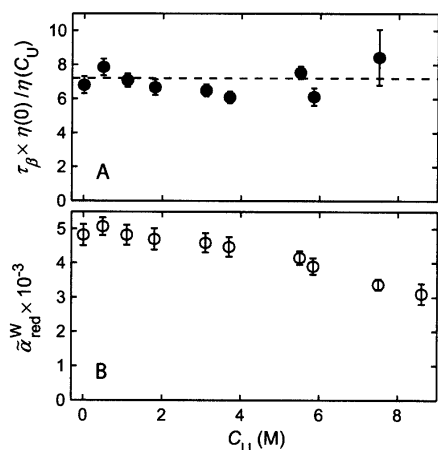


Figure 5. Variation of (A) the viscosity-corrected correlation time τ_β (filled circles) and (B) the apparent surface hydration parameter $\tilde{\alpha}_{\text{red}}^{\text{W}}$ (open circles) during urea-denaturation of 2.3 mM apo I-FABP at pH 7.0 and 27°C. τ_β and $\tilde{\alpha}_{\text{red}}^{\text{W}}$ were derived from single-Lorentzian fits to ¹⁷O MRD profiles. The horizontal line in A corresponds to the independently determined rotational correlation of native I-FABP.

effects of increased surface area and disrupted binding cavity precludes a quantitative analysis of the variation of $\tilde{\alpha}_{\text{red}}^{\text{W}}$ with urea concentration (see Fig. 5B).

Nevertheless, we can extract useful information about the denatured state from the value $\tilde{\alpha}_{\text{red}}^{\text{W}} = (3.1 \pm 0.3) \times 10^3$ obtained at 8.6 M urea, where the cavity is disrupted and $\tilde{\alpha}_{\text{red}}^{\text{W}} = N_{\text{S}}^{\text{W}} \rho_{\text{S}}^{\text{W}}$. We correct for urea competition with the aid of the relation $N_{\text{S}}^{\text{W}} = N_{\text{W}} (1 - \theta)$. The urea-binding constant K_{U} is expected to lie in the range 0.05–0.2 M⁻¹ (Pace 1986; Liepinsh and Otting 1994; Schellman and Gassner 1996; Wu and Wang 1999). For this range, equation 12 yields $\theta = 0.33$ –0.67, whereby $N_{\text{W}} \rho_{\text{S}}^{\text{W}} = (4.6$ –9.4) $\times 10^3$. For $K_{\text{U}} = 0.1$ M⁻¹, $N_{\text{W}} \rho_{\text{S}}^{\text{W}} = (6.2 \pm 0.6) \times 10^3$. A previous MRD study gave a similar value, $N_{\text{W}} \rho_{\text{S}}^{\text{W}} = (5.6 \pm 0.9) \times 10^3$, for bovine α -lactalbumin denatured by guanidinium chloride (Denisov et al. 1999). That protein is nearly the same size as I-FABP (123 versus 131 residues), and $N_{\text{W}} \rho_{\text{S}}^{\text{W}}$ was found to be unaffected by cleavage of the four disulfide bonds (I-FABP has no cysteine).

The experimentally derived $N_{\text{W}} \rho_{\text{S}}^{\text{W}}$ value can be used as a constraint on models of the denatured state. In particular, a fully solvent-exposed polypeptide chain can be ruled out categorically. For this extreme model, the dynamic retardation should be essentially the same as for an aqueous mixture of amino acids, $\rho_{\text{S}}^{\text{W}} = 1.3 \pm 0.1$ (Ishimura and Uedaira 1990; Denisov et al. 1999). Note that, because urea has little effect on water dynamics in the bulk solvent (see Fig. 2), it should have negligible effect on the relative dynamic retardation factor $\rho_{\text{S}}^{\text{W}}$. With this $\rho_{\text{S}}^{\text{W}}$ value and the relation $A_{\text{S}}/\text{nm}^2 = 0.15 N_{\text{W}}$ (see Materials and Methods), the experimental constraint yields for the denatured-state solvent-accessible surface area, $A_{\text{S}}(\text{D}) = 0.15 \times (6.2 \pm 0.6) \times 10^3 / (1.3 \pm 0.1) = 715 \pm 90$ nm². This value greatly exceeds all computational estimates of $A_{\text{S}}(\text{D})$ for unfolded models of I-FABP (Miller et al. 1987; Creamer et al. 1997), ranging from 150 nm² (based on the exposure of the central residue in 17-mer polypeptide segments excised from 43 native protein structures) to 190 nm² (based on the same polypeptide segments in an extended conformation) to 225 nm² (based on extended Gly-Xaa-Gly tripeptides), in all cases with a probe of radius 1.4 Å.

The denatured state of I-FABP must therefore be much more compact than a fully exposed polypeptide chain. It is difficult to be more quantitative, because (solvent-mediated) contacts between polypeptide segments not only reduce N_{W} (or A_{S}), but are also expected to increase $\rho_{\text{S}}^{\text{W}}$. The typical value $\rho_{\text{S}}^{\text{W}} = 4.5$ for native proteins is thought to be strongly dominated by a small number of water molecules in clefts and pockets on the surface, with τ_{S} values of several hundred psec (Denisov and Halle 1996; Halle 1998). For a denatured state without rigid and persistent structural constraints, such special hydration sites are improbable. More likely, denatured I-FABP contains a large number of water molecules that are all substantially more perturbed

than are water molecules at the surface of the native protein because they act as hydrogen-bond cross-links between polypeptide segments in transient clusters.

Persistent urea binding to the native and denatured states of I-FABP

Up to this point, we have only discussed water ¹⁷O MRD data. We now turn to the ²H MRD data, which report on water as well as urea. By explicitly taking into account the slow to intermediate hydrogen exchange between water and urea (Vold et al. 1970; Hunston and Klotz 1971) in the analysis of the magnetization recovery, we could determine the individual water and urea ²H relaxation rates R_1^{W} and R_1^{U} at most of the investigated urea concentrations (see Materials and Methods). These ²H MRD profiles were then subjected to the same single-Lorentzian analysis as the ¹⁷O MRD data.

The reduced parameters $\tilde{\alpha}_{\text{red}}^{\text{W}}$, $\beta_{\text{red}}^{\text{W}}$, and τ_{β} derived from the water ²H MRD profiles, and their dependence on C_{U} , conform closely to the corresponding ¹⁷O parameters. For example, $\beta_{\text{red}}^{\text{W}}$ decreases from 2.2 ± 0.2 in the absence of urea to 0.9 ± 0.3 at $C_{\text{U}} = 7.5$ M (the highest urea concentration investigated by ²H MRD). This agreement indicates that the contribution to R_1^{W} from labile hydrogens in the protein is negligible at pH 7, as previously found for the native state (Wiesner et al. 1999). The agreement between the water ²H and ¹⁷O parameters also supports the protocol used to separate the water and urea contributions to the ²H magnetization recovery (see Materials and Methods).

Figure 6 shows urea ²H dispersion profiles at three urea

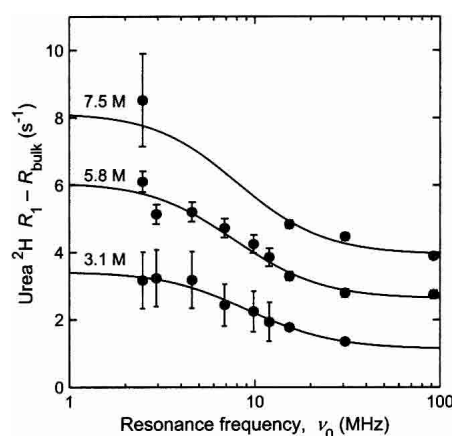


Figure 6. Urea ²H MRD profiles at 27°C in aqueous solutions of 2.3 mM apo I-FABP at pH 7.0 with 3.1–7.5 M urea. The figure shows the excess ²H relaxation rate $R_1^{\text{U}} - R_{\text{bulk}}^{\text{U}}$, normalized to $N_{\text{T}}^{\text{U}} = 1,470$ ($C_{\text{U}} = 3.1$ M) to remove the trivial dependence on urea concentration. The curves were obtained from single-Lorentzian fits and the resulting parameter values are given in Table 3.

concentrations. The reduced parameters resulting from single-Lorentzian fits are collected in Table 3. Within the experimental uncertainty, the viscosity-corrected correlation time τ_β does not deviate significantly from the water ^{17}O correlation time (see Fig. 5A). As in the case of the water ^{17}O and ^2H dispersions, we can therefore identify τ_β with the tumbling time τ_R of the protein. This means that the species giving rise to the urea ^2H dispersion has a residence time longer than 10 nsec. In principle, this species could be either bound urea or labile hydrogens in the protein.

A labile-hydrogen contribution to R_1^U can be ruled for the following reasons. First, the labile-hydrogen contribution to $\beta_{\text{red}}^W(^2\text{H})$ was found to be negligible, and in β_{red}^U such a contribution is further reduced by a factor 2 because urea contains twice as many hydrogens as water. Second, sufficiently fast (meaning submillisecond) exchange of labile hydrogens between I-FABP and urea, whether direct or via water, requires catalysis by an ionized species. In the indirect pathway, H_3O^+ and OH^- catalyze both the protein \rightarrow water and the water \rightarrow urea proton transfer steps. At pH 7, the second step occurs on a time scale of 1 sec (see Materials and Methods), thus effectively eliminating this pathway for magnetization transfer. The direct pathway would presumably be catalyzed by $\text{H}_2\text{NCONH}_3^+$, which is present at similarly low concentration as H_3O^+ (protonated urea has a $\text{p}K_a$ of 0.1), and is likely to be a less potent catalyst. Consistent with these arguments, exchange between protein and urea was shown to be slow on the NOESY mixing time scale (40 msec) in an intermolecular NOE study of BPTI at pH 7 (Liepinsh and Otting 1994).

On the basis of these considerations, we conclude that the urea ^2H dispersion, observed at all investigated urea concentrations from 3.1 to 7.5 M, demonstrates that urea binds to I-FABP with a residence time longer than 10 nsec but shorter than ca. 0.2 msec (the intrinsic relaxation time of urea bound to I-FABP; see Materials and Methods). To our knowledge, this is the first demonstration of such long-lived urea binding to proteins. The dispersion could result from urea molecules trapped in the binding cavity, but then β_{red}^U should decrease with increasing urea concentration and vanish at $C_U = 7.5$ M, where the CD data indicate that the cavity is disrupted (see Fig. 4). In contrast, we find that β_{red}^U increases with C_U (see Table 3), indicating that urea binds

to specific sites in (or on) the native as well as the denatured protein. Because trapping in the large cavity is apparently not involved, we may write $\beta_{\text{red}}^U = \theta_I \mathcal{N}_{I,U} S_{I,U}^2$, where $\mathcal{N}_{I,U}$ is the number of long-lived (specific) urea-binding sites, θ_I their mean occupancy, and $S_{I,U}$ the orientational order parameter of the bound urea molecule(s). The latter two factors cannot exceed unity, so the β_{red}^U values in Table 3 imply that both the native and denatured forms of I-FABP contain at least one specific urea-binding site.

The increase of β_{red}^U with C_U does not necessarily indicate a higher affinity for urea in the denatured state, but can be explained by mass action even if the native and denatured states have the same number of specific binding sites with the same urea binding constant. With $K_U = 0.1 \text{ M}^{-1}$, equation 12 yields a twofold higher occupancy θ_I at 7.5 M than at 3.1 M urea. (The maximum in β_{red}^U at $C_U = 5.5$ M may be a systematic error; the product $\beta_{\text{red}}^U \tau_\beta$ increases monotonically with C_U .) On the other hand, a residence time longer than 10 nsec implies that $K_U > 1 \times 10^{-8} k_{\text{on}}$, where k_{on} is the second-order association rate constant. If urea binding is close to diffusion controlled and/or if the residence time is much longer than 10 nsec, so that $K_U \gg 1 \text{ M}^{-1}$, then the long-lived urea binding site(s) will be essentially saturated at the investigated urea concentrations. The increase of β_{red}^U with C_U would then suggest a larger number of long-lived urea-binding sites in the denatured state. In any event, the observation of long-lived urea binding to the native and denatured states of I-FABP raises the possibility that strong urea binding contributes significantly to the unfolding thermodynamics and thereby calls into question the validity of the linear extrapolation method widely used to determine the stability of the native protein in the absence of urea (Myers et al. 1995).

Urea-protein interactions have also been studied by other NMR methods than MRD, in particular, intermolecular NOEs and chemical-shift titration. In a study of the small stable protein BPTI, which retains its native structure up to 8 M urea, four urea binding sites were detected in surface pockets and grooves (Liepinsh and Otting 1994) with $K_U = 0.2 \text{ M}^{-1}$ and residence times of a few nsec at 4°C. In a similar study of the urea-unfolded (7 M) state of the DNA-binding domain of the 434-repressor at -8°C (Dötsch et al. 1995; Dötsch 1996), positive NOESY cross-peaks were observed between urea and most aliphatic protons, indicating urea residence times longer than 0.3 nsec. In both studies, the urea cross-peaks vanished at higher temperatures without exhibiting the expected sign reversal. It should be noted that the model used to transform the sign of the cross-peak into a bound on the residence time may not be appropriate for denatured proteins.

Transient urea interactions with the protein surface during denaturation of I-FABP

The high urea concentrations needed to denature proteins implies that weak binding to many sites is involved. Infor-

Table 3. Results derived from urea ^2H MRD parameters

| C_U (M) | τ_β (ns) | β_{red}^U | $\tilde{\alpha}_{\text{red}}^U \times 10^{-3}$ | $\mathcal{N}_U \rho_S^U \times 10^{-3a}$ |
|-----------|-------------------|------------------------|--|--|
| 3.1 | 10 ± 3 | 0.5 ± 0.1 | 0.44 ± 0.04 | 1.9 ± 0.2 |
| 3.7 | 10 ± 3 | 0.6 ± 0.1 | 0.36 ± 0.06 | 1.4 ± 0.2 |
| 5.5 | 8 ± 2 | 1.0 ± 0.1 | 0.76 ± 0.07 | 2.1 ± 0.2 |
| 5.8 | 12 ± 2 | 0.7 ± 0.1 | 0.94 ± 0.08 | 2.5 ± 0.2 |
| 7.5 | 11 ± 3 | 0.9 ± 0.1 | 1.32 ± 0.10 | 2.9 ± 0.2 |

^a Based on $\tilde{\alpha}_{\text{red}}^U = \mathcal{N}_S^U \rho_S^U = \mathcal{N}_U \theta \rho_S^U$, with θ obtained from equation 12 with $K_U = 0.1 \text{ M}^{-1}$.

mation about such interactions is contained in the parameter $\tilde{\alpha}_{\text{red}}^{\text{U}}$ (see Table 3). Having rejected the possibility of urea trapping in the large cavity, we can attribute this parameter entirely to urea molecules in short-lived (<1 nsec) association with the external protein surface, so that $\tilde{\alpha}_{\text{red}}^{\text{U}} = N_{\text{U}}\rho_{\text{S}}^{\text{U}} = N_{\text{U}}\theta\rho_{\text{S}}^{\text{U}}$. To rationalize the observed variation of $\tilde{\alpha}_{\text{red}}^{\text{U}}$ with C_{U} , we write

$$\tilde{\alpha}_{\text{red}}^{\text{U}} = \theta[fN_{\text{U}}(N)\rho_{\text{S}}^{\text{U}}(N) + (1-f)N_{\text{U}}(D)\rho_{\text{S}}^{\text{U}}(D)] \quad (2)$$

with the mean urea occupancy $\theta(C_{\text{U}})$ given by equation 12 (with the same binding constant K_{U} for the native and denatured states) and the native protein fraction $f(C_{\text{U}})$ obtained from equation 11. The parameters m and $C_{1/2}$ may be taken from either the CD or the $\beta_{\text{red}}^{\text{W}}$ (^{17}O) denaturation curve (see Fig. 4; Table 2). Because the available $\tilde{\alpha}_{\text{red}}^{\text{U}}$ data do not allow us to determine all of the three remaining parameters, we fix the value of K_{U} . Acceptable fits are obtained for binding constants in the plausible range 0.05–0.2 M^{-1} (see Fig. 7). For this K_{U} range, the ratio of the two adjustable parameters is $N_{\text{U}}(D)\rho_{\text{S}}^{\text{U}}(D)/N_{\text{U}}(N)\rho_{\text{S}}^{\text{U}}(N) = 1.8 \pm 0.3$. For water, the corresponding ratio is 3.0 ± 0.3 if $K_{\text{U}} = 0.1 \text{ M}^{-1}$.

The fit in Figure 7 yields $N_{\text{U}}(D)\rho_{\text{S}}^{\text{U}}(D) = (3.3 \pm 0.3) \times 10^3$ for $K_{\text{U}} = 0.1 \text{ M}^{-1}$. This may be compared with the corresponding water ^{17}O result, $N_{\text{U}}(D)\rho_{\text{S}}^{\text{W}}(D) = (6.2 \pm 0.6) \times 10^3$, obtained with the same K_{U} . If we assume that $\rho_{\text{S}}^{\text{U}}(D) = \rho_{\text{S}}^{\text{W}}(D)$, we can regard the ratio of these numbers as the ratio of water to urea binding sites on the surface of the denatured protein, that is, $N_{\text{U}}(D)/N_{\text{U}}(N) = 1.9 \pm 0.3$. If water and urea compete for the same space at the polypep-

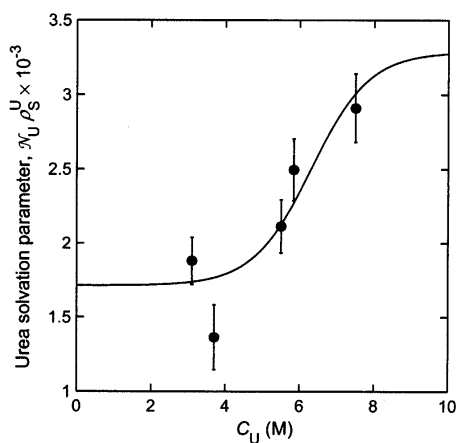


Figure 7. Variation of urea–protein interactions during urea-denaturation of 2.3 mM apo I-FABP at pH 7.0 and 27°C. The parameter $N_{\text{U}}\rho_{\text{S}}^{\text{U}}$ was obtained from the urea ^2H MRD parameter $\tilde{\alpha}_{\text{red}}^{\text{U}}$ after division by the fractional urea occupancy θ , calculated from the solvent exchange model with $K_{\text{U}} = 0.1 \text{ M}^{-1}$ (see Table 3). The curve resulted from a fit where the value of $N_{\text{U}}\rho_{\text{S}}^{\text{U}}$ in the native and denatured states were adjusted, while the parameters m and $C_{1/2}$ characterizing the $\text{N} \leftrightarrow \text{D}$ equilibrium were fixed at the values deduced from the $\beta_{\text{red}}^{\text{W}}$ (^{17}O) denaturation curve (see Fig. 4).

ptide surface, this should equal the ratio $a_{\text{U}}/a_{\text{W}}$ of areas occupied by single urea and water molecules at the surface. The latter ratio can be approximated as $(\bar{V}_{\text{U}}/\bar{V}_{\text{W}})^{2/3}$. The ratio of partial molar volumes varies from 2.45 to 2.55 in our C_{U} range (Gucker et al. 1938). With $\bar{V}_{\text{U}}/\bar{V}_{\text{W}} = 2.5$, we get $a_{\text{U}}/a_{\text{W}} = 1.8$. The urea ^2H and water ^{17}O MRD data are thus consistent with a similarly large dynamic retardation for urea and water.

To summarize, the urea ^2H and water ^{17}O MRD data support a picture of the denatured state where much of the polypeptide chain participates in clusters that are more compact and more ordered than a random coil, but nevertheless, are penetrated by large numbers of water and urea molecules. These solvent-penetrated clusters must be sufficiently compact to allow side chains from different polypeptide segments to come into hydrophobic contact, while, at the same time, permitting solvent molecules to interact favorably with peptide groups and with charged and polar side chains. The exceptional hydrogen-bonding capacity and small size of water and urea molecules are likely to be essential attributes in this regard. In such clusters, many water and urea molecules will simultaneously interact with more than one polypeptide segment, and their rotational motions will therefore be more strongly retarded than at the surface of the native protein. Although the hydrogen-bonding capacity per unit volume is similar for water and urea, the 2.5-fold larger volume of urea reduces the entropic penalty for confining a certain volume of solvent to a cluster. The energetics and dynamics of solvent included in clusters is expected to differ considerably from solvent at the surface of the native protein. This view is supported by the slow water and urea rotation in the denatured state, as deduced from the present MRD data. Further studies are needed to test and refine this tentative picture of the denatured state and to establish whether it applies to a wider range of proteins and denaturing conditions.

Materials and methods

Preparation and characterization of protein solutions

Recombinant apo I-FABP was expressed, purified, and delipidated as previously described (Kurian 1998; Wiesner et al. 1999). Lyophilized protein was dissolved in ^2H and ^{17}O enriched water (52 atom % ^2H , 17 atom % ^{17}O) with 10 mM phosphate buffer. A small fraction insoluble protein was removed by centrifugation. The pH (uncorrected for isotope effects) was 7.00 ± 0.05 in all samples.

The protein concentration was determined, with an estimated accuracy of 5%, from absorbance measurements at 280 nm, using an extinction coefficient of $18.6 \text{ mM}^{-1}\text{cm}^{-1}$, calibrated against the complete amino acid analyses performed by Wiesner et al. (1999). Three samples were used for MRD measurements, with I-FABP concentration $C_{\text{p}} = 2.3\text{--}2.4 \text{ mM}$ (see Table 1). The total number of water molecules per protein molecule was obtained as $N_{\text{T}}^{\text{W}} = (1/[6.022 \times 10^{-7} \times C_{\text{p}}/\text{mM}] - V_{\text{p}}/\text{\AA}^3)/(V_{\text{W}}/\text{\AA}^3)$, where $V_{\text{p}} = 18,600$

\AA^3 is the solvent-excluded protein volume, determined with the program GRASP (Nicholls et al. 1993), and $V_w = M_w/(\rho_w N_A) = 30 \text{\AA}^3$ is the volume occupied by a single bulk water molecule.

Urea (BDH, ultrapure) was added directly to the NMR samples, and its molar concentration C_U was determined from the mass of added urea and the volume of the solution. The pH increase caused by addition of urea was corrected by addition of small volumes of HCl. Because N_T^W is the ratio between the numbers of water and protein molecules in the sample, it does not change on addition of urea. The total number N_T^U of urea molecules per protein molecule was obtained by multiplying N_T^W with the factor $x_U/(1-x_U)$, where x_U is the mole fraction urea in the solvent. To obtain the mole fraction x_U from the molarity C_U , we used the following empirical relation for the density d of aqueous urea solutions (Gucker et al. 1938): $d/d_0 = 1 + 1.60155 \times 10^{-2} C_U - 1.4000 \times 10^{-4} C_U^2 + 2.601 \times 10^{-6} C_U^3$, with $d_0 = 0.997 \text{ g cm}^{-3}$ the density of pure H_2O at 25°C . Note that the relation between x_U and C_U is essentially independent of H/D isotope substitution. Table 1 lists C_U , x_U , and N_T^U for the investigated samples.

Far-UV (216 and 222 nm) circular dichroism (CD) denaturation profiles were recorded at 27°C on a Jasco J-720 spectropolarimeter equipped with a Peltier thermostat, using a cell length of 1 mm. The CD samples (pH 7.0) were prepared by mixing a protein solution (approximately 0.2 mM) with appropriate volumes of 10 mM phosphate buffer with or without 10 M urea. The final protein concentration was $9.7 \mu\text{M}$.

Magnetic relaxation dispersion measurements

Magnetic relaxation dispersion profiles of the ^2H and ^{17}O longitudinal relaxation rate $R_1 = 1/T_1$ were acquired for each of the 10 samples. Each dispersion profile comprised nine magnetic field strengths, accessed with the aid of four different NMR spectrometers, including Varian 600 Unity Plus, Bruker Avance DMX 100, and DMX 200 spectrometers and a field-variable iron-core magnet (Drusch EAR-35N) equipped with a field-variable lock and flux stabilizer and interfaced to a Bruker MSL 100 console. The ^{17}O resonance frequencies ranged from 2.2 to 81.4 MHz and the ^2H frequencies from 2.5 to 92.1 MHz. The sample temperature was adjusted to $27.0 \pm 0.1^\circ\text{C}$ by a thermostated airflow and was checked with a copper-constantan thermocouple referenced to an ice bath.

The relaxation time T_1 was measured by the inversion recovery method, using a 16-step phase cycle, 20 delay times in random order, and a sufficient number of transients to obtain a signal-to-noise ratio of at least 100 (Halle et al. 1999). The ^{17}O magnetization recovered as a single exponential and T_1 was determined from the standard three-parameter fit. The accuracy of $R_1(^{17}\text{O})$ is estimated to $\pm 0.5\%$ (one standard deviation).

Hydrogen exchange between water and urea makes the ^2H magnetization recovery bi-exponential. In the absence of exchange, the water and urea ^2H magnetizations are assumed to relax exponentially with intrinsic relaxation rates R_1^W and R_1^U . In the presence of exchange, the nonequilibrium longitudinal magnetization $\Delta M(t) = M_z(t) - M_0$ in the two states then evolves according to (Slichter 1989)

$$\frac{d}{dt} \Delta M^W(t) = R_1^W \Delta M^W(t) - k_1 \Delta M^W(t) + k_{-1} \Delta M^U(t) \quad (3a)$$

$$\frac{d}{dt} \Delta M^U(t) = R_1^U \Delta M^U(t) - k_{-1} \Delta M^U(t) + k_1 \Delta M^W(t) \quad (3b)$$

This can be written succinctly as

$$\frac{d}{dt} \Delta \mathbf{M}(t) = (\mathbf{R} - \mathbf{K}) \Delta \mathbf{M}(t) \quad (4)$$

where $\Delta \mathbf{M}$ is a column vector formed from the two magnetizations, \mathbf{R} is a diagonal relaxation matrix with elements R_1^W and R_1^U , and \mathbf{K} is an exchange rate matrix with rows $[-k_1 \ k_{-1}]$ and $[k_1 \ -k_{-1}]$. Because the forward and backward rates must balance at equilibrium, the rate constants are not independent: $k_1(1 - P_U) = k_{-1}P_U$. The urea-deuteron fraction P_U is related to the urea mole fraction x_U as $P_U = 2x_U/(1+x_U)$. The single independent rate parameter is conveniently chosen as the overall exchange rate $k_{\text{ex}} = k_1 + k_{-1}$.

The formal solution to equation 4 is $\Delta \mathbf{M}(t) = \mathbf{S} \exp(-\mathbf{D}t) \mathbf{S}^{-1} \Delta \mathbf{M}(0)$, where \mathbf{S} is the matrix that diagonalizes $(\mathbf{R} - \mathbf{K})$, that is, $\mathbf{D} = \mathbf{S}^{-1}(\mathbf{R} - \mathbf{K})\mathbf{S}$. The nonequilibrium magnetization present immediately after the 180° pulse is described by the vector $\Delta \mathbf{M}(0) = -\mathbf{M}_0(1 + \phi)$, where $\phi = 1$ for an ideal 180° pulse and the elements of \mathbf{M}_0 can be identified with the relative equilibrium populations P_U and $1 - P_U$. Finally, the observed water and urea ^2H magnetizations are computed from $M^W(t) = \sigma^W [\Delta M^W(t) + M_0^W]$ and the analogous relation for $M^U(t)$, with instrumental scaling factors σ^W and σ^U . At magnetic fields below 2 T, the water and urea resonances could not be resolved. At these fields, we analyzed the total magnetization $M^W + M^U$, taking ϕ and σ to be the same for water and urea. At the three highest fields, separate relaxation experiments were performed on the two resonances, with independent ϕ and σ parameters and different sets of relaxation delays.

The combined water and urea inversion recovery data recorded at all fields were fitted simultaneously with P_U and k_{ex} as common parameters and R_1^W , R_1^U , $\phi^{W/U}$, and $\sigma^{W/U}$, and as field-dependent parameters (but with common ϕ and σ at low fields). In a typical case, we thus fitted 44 parameters to 240 data points. Figure 8 shows that this bi-exponential fit substantially improves upon a single-exponential fit. The P_U values deduced from the fits agree quantitatively with the urea-deuteron fractions calculated from sample compositions (see Table 1). The rate constants k_{-1} obtained

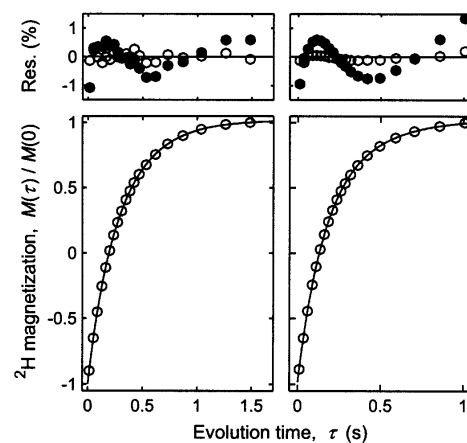


Figure 8. Fits to ^2H inversion recovery data from an apo I-FABP solution containing 5.8 M urea. (Left) Sum of the water and urea magnetizations at 0.45 T. (Right) Urea magnetization at 4.7 T. In both panels, the curves resulted from a simultaneous fit to data from all nine magnetic fields. The residuals shown in the upper panels are the differences (in percent) between measured and calculated $M(t)$ for an individual three-parameter single-exponential fit (filled circles) and for the simultaneous bi-exponential fit (open circles).

from the fits range from 0.87 sec⁻¹ at 3.1 M to 1.22 sec⁻¹ at 7.5 M urea, in agreement (considering differences in temperature and H/D isotope composition) with previous results (Vold et al. 1970; Hunston and Klotz 1971). The observed increase in k_{-1} with urea concentration is consistent with the report that acid catalysis is no longer first order in urea concentration above 3 M (Vold et al. 1970). The accuracy of R_1^W and R_1^U obtained from these fits is estimated to $\pm(0.5\text{--}1.0)\%$ (one standard deviation) at the three highest fields, with somewhat inferior accuracy at lower fields.

Using the protocol described above, we extracted the ²H relaxation rates R_1^W and R_1^U at urea concentrations from 3.1 to 7.5 M (no ²H measurements were done at 8.6 M). In addition, R_1^W was determined at $C_U = 0$ and 0.5 M, where the urea contribution to the observed R_1 is negligible. At $C_U = 1.1$ and 1.8 M, we could not separate R_1^W and R_1^U because of the small urea-deuteron fraction ($P_U \approx 0.05$).

²H relaxation experiments on protein-free reference samples were carried out at 3.1 M, 5.5 M, and 7.5 M urea at the three highest fields, to obtain R_1^W and R_1^U . By fitting the measured R_1^W and R_1^U rates to cubic polynomials, the bulk relaxation rates were then recalculated at all investigated urea concentrations. For R_1^W , we also included the relaxation rates at 0 M and 0.5 M urea in the fit. Considering the spread in the data at the investigated concentrations, the error introduced this way is less than 1% for R_1^W and around 2% for R_1^U .

Analysis of magnetic relaxation dispersion data

All magnetic relaxation dispersion (MRD) profiles were analyzed with an in-house Matlab implementation of the Levenberg-Marquardt nonlinear χ^2 minimization algorithm (Press et al. 1992). To estimate the uncertainty in the fitted parameters, we performed fits on a Monte Carlo generated ensemble of 1000 data sets, subject to random Gaussian noise with 0.5% standard deviation for the ¹⁷O data. For the ²H data, the standard deviations were set equal to the estimates made above. Quoted uncertainties correspond to a confidence level of 68.3% (one standard deviation).

The water ¹⁷O and ²H MRD profiles, $R_1(\omega_0)$, were modeled by a bi-Lorentzian spectral density $J(\omega_0)$ according to (Halle et al. 1999; Wiesner et al. 1999; Halle and Denisov 2001)

$$R_1(\omega_0) = R_{\text{bulk}} + 0.2 J(\omega_0) + 0.8 J(2\omega_0) \quad (5)$$

$$J(\omega_0) = \alpha + \frac{\beta \tau_\beta}{1 + (\omega_0 \tau_\beta)^2} + \frac{\gamma \tau_\gamma}{1 + (\omega_0 \tau_\gamma)^2} \quad (6)$$

where $\omega_0 = 2\pi \nu_0$ is the resonance frequency in angular frequency units and R_{bulk} is the relaxation rate of the bulk solvent. The five adjustable parameters in equation 6 were interpreted according to the dynamic cluster model (Modig et al. 2003), a generalization of the standard model (Halle et al. 1999; Halle and Denisov 2001) adapted to proteins with large water-filled internal cavities. This model distinguishes three types of protein-associated water: (1) water molecules in contact with the protein surface (subscript S) are responsible for the frequency-independent α term, (2) singly buried internal water molecules (subscript I) give rise to the dispersive β term, and (3) water molecules trapped in the large binding cavity (subscript C) account for the dispersive γ term.

The parameters in equation 6 are related to the molecular parameters of the model in the following way (Modig et al. 2003):

$$\alpha = \frac{R_{\text{bulk}}}{N_T^W} N_S^W \rho_S^W \quad (7a)$$

$$\beta = \frac{\omega_Q^2}{N_T^W} (N_I^W S_{I,W}^2 + N_C^W S_{C,W}^2 A_{C,W}^2) \quad (7b)$$

$$\gamma = \frac{\omega_Q^2}{N_T^W} N_C^W S_{C,W}^2 (1 - A_{C,W}^2) \quad (7c)$$

$$\tau_\beta = \tau_R \quad (7d)$$

$$\tau_\gamma = \left[\frac{1}{\tau_R} + \frac{N_C^W}{(N_C^W - 1) \tau_S} \right]^{-1} \quad (7e)$$

Here, ω_Q is the rigid-lattice ¹⁷O or ²H quadrupole coupling frequency in a protein-bound water molecule, and N_T^W is the total number of water molecules per protein molecule, which is a measure of the protein concentration (see above). $\omega_Q = 76.1 \times 10^5$ rad sec⁻¹ for ¹⁷O and 8.70×10^5 rad sec⁻¹ for ²H (Halle et al. 1999). The index W serves to distinguish water parameters from analogous urea parameters (see below).

In equation 7a, N_S^W is the number of water molecules in contact with the protein surface, estimated by dividing the solvent-accessible surface area A_S of the protein with the effective area occupied by a water molecule, usually taken as 0.15 nm² (Halle et al. 1999). For native I-FABP, $A_S = 69$ nm² (Wiesner et al. 1999), giving $N_S^W = 460$. On average, these surface waters have a longer rotational correlation time τ_S than in bulk water (τ_{bulk}), and this is expressed by the dynamic retardation factor $\rho_S^W = \tau_S/\tau_{\text{bulk}} - 1$.

The β dispersion is produced by a small number N_I^W of singly buried water molecules along with a larger number N_C^W of water molecules trapped in the large fatty acid binding cavity. The residence times of all these water molecules, τ_I in singly occupied small cavities and τ_C in the large cavity, are much longer than the rotational correlation time τ_R of the protein, from which follows equation 7d. The root-mean-square orientational order parameter $S_{I,W}$ for internal waters is close to 1, whereas $S_{C,W}$ is smaller. Unlike the internal waters, which are highly localized until they exchange with external water, the cavity waters exchange among hydration sites within the large cavity. This intracavity exchange is responsible for the γ dispersion, and introduces two additional parameters: the mean residence time τ_{SC} in a particular hydration site, and the cavity order parameter A_C , which characterizes the orientational distribution of the hydration sites in the cavity.

Because $\tau_\gamma \approx 1$ nsec, the γ dispersion is not fully characterized by relaxation data extending up to 80–90 MHz. In fact, at all points on the dispersion profile except the highest frequency, the γ contribution can be accurately described by its low-frequency (extreme narrowing) limit. If the highest frequency point is omitted, the MRD data can thus be described with a single-Lorentzian spectral density function, comprising the β dispersion in equation 6 and a renormalized α parameter

$$\tilde{\alpha} = \alpha + \gamma \tau_\gamma \quad (8)$$

The model described here is valid in the fast-exchange regime on the relaxation time scale, defined by the inequality $\tau_I, \tau_C \ll (\omega_Q^2 S^2 \tau_R)^{-1}$ (Halle et al. 1999; Halle and Denisov 2001). For a highly ordered water molecule (say, $S = 0.9$) in a protein with $\tau_R = 7$ nsec, this means that $\tau_I, \tau_C \ll 3$ μ sec. A β dispersion with $\tau_\beta = \tau_R$ thus provides lower and upper bounds on the two residence times: $\tau_R \ll \tau_I, \tau_C \ll (\omega_Q^2 S^2 \tau_R)^{-1}$.

Urea ²H MRD data can be analyzed with the same model expressions as described above for water ²H and ¹⁷O data. The index W is then replaced by U. For example, N_T^U is the total number of

urea molecules per protein molecule (see above). The ^2H quadrupole coupling frequency in urea is expressed as $\omega_Q^2 = 3\pi^2\chi^2(1 + \eta^2/3)/2$, where χ and η are the quadrupole coupling constant and asymmetry parameter, respectively (Slichter 1989). From solid-state NMR studies of a urea single-crystal, $\chi = 211.5 \pm 0.7$ kHz and $\eta = 0.144 \pm 0.002$ (Chiba 1965; Heaton et al. 1989), yielding $\omega_Q = 8.17 \times 10^5$ rad sec $^{-1}$.

Modeling of urea concentration dependence

In the investigated protein solutions, water and urea molecules exchange rapidly (on the relaxation time scale) between solvation sites on native (N) and denatured (D) protein molecules and the bulk solvent region. The observed MRD parameters α , β , and γ are therefore population-weighted averages. For example,

$$\beta = f\beta(N) + (1-f)\beta(D) \quad (9)$$

where f is the fraction native protein. Similarly, τ_β is the effective correlation time resulting from a single-Lorentzian fit to the—possibly bi-Lorentzian— β dispersion

$$J_\beta(\omega_0) = \frac{f\beta(N)}{\beta} \frac{\tau_\beta(N)}{1 + [\omega_0\tau_\beta(N)]^2} + \frac{(1-f)\beta(D)}{\beta} \frac{\tau_\beta(D)}{1 + [\omega_0\tau_\beta(D)]^2} \quad (10)$$

In practice, the deviation from a single Lorentzian is undetectably small, as expected if $\beta(D) \ll \beta(N)$ or if $\tau_\beta(N) \approx \tau_\beta(D)$.

To obtain the dependence of the native protein fraction f on the urea concentration C_U , we make the usual assumption that the free energy of denaturation varies linearly with C_U (Pace 1986). It then follows that $f = 1/(1 + K_D)$, with the denaturation constant K_D given by

$$K_D = \exp\left[\frac{m}{RT}(C_U - C_{1/2})\right] \quad (11)$$

where the parameters $C_{1/2}$ and m characterize the midpoint and slope, respectively, of the $N \rightarrow D$ transition.

The urea concentration not only controls the $N \leftrightarrow D$ equilibrium; it also affects the number of water (N_S^W) and urea (N_S^U) molecules in contact with the protein surface. The molecular parameters $N_S^W \rho_S^W$ and $N_S^U \rho_U^W$ derived from the MRD parameter α by means of equation 7a can be decomposed as in equation 10, but now also the numbers N_S^W and N_S^U depend on C_U . We describe this dependence with the aid of the solvent exchange model (Schellman 1990, 1994), where urea binding to the protein surface is described thermodynamically as a one-to-one exchange with water. The urea occupancy averaged over all binding sites is then given by

$$\theta = \frac{K_U a_U^c}{a_W^x + K_U a_U^c} \quad (12)$$

where K_U is an effective urea binding constant (with units M^{-1}), a_U^c is the urea activity on the molarity scale, and a_W^x is the water activity on the mole fraction scale. We then write $N_S^U(N) = N_U(N)\theta(N)$ and $N_S^W(N) = N_W(N)[1 - \theta(N)]$ along with analogous expressions for the denatured (D) state. Here, $N^U(N)$ and $N^W(N)$ are the number of sites on the surface of the native protein that can be occupied by urea and water molecules, respectively. Because urea is a larger molecule than water, we allow these numbers to be different. This may be regarded as an ad hoc generalization of the

one-to-one solvent exchange model. We obtain the activities from the following cubic polynomials, fitted to experimental data covering the C_U range 0–7.8 M at 25°C (Stokes 1967; Schellman and Gassner 1996),

$$a_W^x = 1 - 1.8034 \times 10^{-2} C_U + 9.629 \times 10^{-5} C_U^2 - 5.575 \times 10^{-5} C_U^3 \quad (13a)$$

$$a_U^c/C_U = 1 - 3.8990 \times 10^{-2} C_U + 5.2295 \times 10^{-3} C_U^2 - 1.522 \times 10^{-4} C_U^3 \quad (13b)$$

Acknowledgments

We thank Vladimir Denisov and Hans Lilja for spectrometer assistance. This work was supported by the Crafoord Foundation and the Swedish Research Council.

The publication costs of this article were defrayed in part by payment of page charges. This article must therefore be hereby marked “advertisement” in accordance with 18 USC section 1734 solely to indicate this fact.

References

- Åstrand, P.-O., Wallqvist, A., and Karlström, G. 1994. Molecular dynamics simulations of 2 *m* aqueous urea solutions. *J. Phys. Chem.* **98**: 8224–8233.
- Bagno, A., Lovato, G., Scorrano, G., and Wijnen, J.W. 1993. Solvation of nonelectrolytes in water probed by ^{17}O relaxation of the solvent. *J. Phys. Chem.* **97**: 4601–4607.
- Bakowies, D. and van Gunsteren, W.F. 2002. Simulations of apo and holo-fatty acid binding protein: Structure and dynamics of protein, ligand and internal water. *J. Mol. Biol.* **315**: 713–736.
- Banaszak, L., Winter, N., Xu, Z., Bernlohr, D.A., Cowan, S., and Jones, A.T. 1994. Lipid-binding proteins: A family of fatty acid and retinoid transport proteins. *Adv. Protein Chem.* **45**: 89–151.
- Burns, L.L., Dalessio, P.M., and Ropson, I.J. 1998. Folding mechanism of three structurally similar β -sheet proteins. *Proteins* **33**: 107–118.
- Cafilisch, A. and Karplus, M. 1999. Structural details of urea binding to barnase: A molecular dynamics analysis. *Structure* **7**: 477–488.
- Capaldi, A.P. and Radford, S.E. 1998. Kinetic studies of β -sheet protein folding. *Curr. Opin. Struct. Biol.* **8**: 86–92.
- Chattopadhyay, K., Saffarian, S., Elson, E.L., and Frieden, C. 2002a. Measurement of microsecond dynamic motion in the intestinal fatty acid binding protein by using fluorescence correlation spectroscopy. *Proc. Natl. Acad. Sci.* **99**: 14171–14176.
- Chattopadhyay, K., Zhong, S., Yeh, S.R., Rousseau, D.L., and Frieden, C. 2002b. The intestinal fatty acid binding protein: The role of turns in fast and slow folding processes. *Biochemistry* **41**: 4040–4047.
- Chiba, T. 1965. A deuteron magnetic resonance study of urea- d_4 . *Bull. Chem. Soc. Jpn.* **38**: 259–263.
- Choy, W.-Y., Mulder, F.A.A., Crowhurst, K.A., Muhandiram, D.R., Millett, I.S., Doniach, S., Forman-Kay, J., and Kay, L.E. 2002. Distribution of molecular size within an unfolded state ensemble using small-angle X-ray scattering and pulse field gradient NMR techniques. *J. Mol. Biol.* **316**: 101–112.
- Clark, P.L., Liu, Z.-P., Rizo, J., and Gierasch, L.M. 1997. Cavity formation before stable hydrogen bonding in the folding of a β -clam protein. *Nat. Struct. Biol.* **4**: 883–886.
- Clark, P.L., Weston, B.F., and Gierasch, L.M. 1998. Probing the folding pathway of a β -clam protein with single-tryptophan constructs. *Fold. Design* **3**: 401–412.
- Creamer, T.P., Srinivasan, R., and Rose, G.D. 1997. Modeling unfolded states of proteins and peptides. II. Backbone solvent accessibility. *Biochemistry* **36**: 2832–2835.
- Dalessio, P.M. and Ropson, I.J. 1998. pH dependence of the folding of intestinal fatty acid binding protein. *Arch. Biochem. Biophys.* **359**: 199–208.
- . 2000. β -Sheet proteins with nearly identical structures have different folding intermediates. *Biochemistry* **39**: 860–871.
- Denisov, V.P. and Halle, B. 1995. Hydrogen exchange and protein hydration:

- The deuterium spin relaxation dispersions of bovine pancreatic trypsin inhibitor and ubiquitin. *J. Mol. Biol.* **245**: 698–709.
- . 1996. Protein hydration dynamics in aqueous solution. *Faraday Discuss.* **103**: 227–244.
- . 1998. Thermal denaturation of ribonuclease A characterized by water ^{17}O and ^2H magnetic relaxation dispersion. *Biochemistry* **37**: 9595–9604.
- Denisov, V.P., Peters, J., Hörlein, H.D. and Halle, B. 1996. Using buried water molecules to explore the energy landscape of proteins. *Nat. Struct. Biol.* **3**: 505–509.
- Denisov, V.P., Jonsson, B.-H. and Halle, B. 1999. Hydration of denatured and molten globule proteins. *Nat. Struct. Biol.* **6**: 253–260.
- Dill, K.A. and Shortle, D. 1991. Denatured states of proteins. *Annu. Rev. Biochem.* **60**: 795–825.
- Dötsch, V. 1996. Characterization of protein–solvent interactions with NMR-spectroscopy: The role of urea in the unfolding of proteins. *Pharm. Acta Helv.* **71**: 87–96.
- Dötsch, V., Wider, G., Siegal, G., and Wüthrich, K. 1995. Interaction of urea with an unfolded protein. The DNA-binding domain of the 434-repressor. *FEBS Lett.* **366**: 6–10.
- Ellerton, H.D. and Dunlop, P.J. 1966. Activity coefficients for the systems water-urea and water-urea-sucrose at 25° from isopiestic measurements. *J. Phys. Chem.* **70**: 1831–1837.
- Frolov, A. and Schroeder, F. 1997. Time-resolved fluorescence of intestinal and liver fatty acid binding proteins: Role of fatty acyl CoA and fatty acid. *Biochemistry* **36**: 505–517.
- Gucker, F.T., Gage, F.W., and Moser, C.E. 1938. The densities of aqueous solutions of urea at 25 and 30° and the apparent molal volume of urea. *J. Am. Chem. Soc.* **60**: 2582–2588.
- Halle, B. 1998. Water in biological systems: The NMR picture. In *Hydration processes in biology* (ed. M.-C. Bellissent-Funel), pp. 233–249. IOS Press, Amsterdam.
- Halle, B. and Denisov, V.P. 2001. Magnetic relaxation dispersion studies of biomolecular solutions. *Methods Enzymol.* **338**: 178–201.
- Halle, B., Denisov, V.P., and Venu, K. 1999. Multinuclear relaxation dispersion studies of protein hydration. In *Biological magnetic resonance* (eds. N.R. Krishna and L.J. Berliner), Vol. 17, pp. 419–484. Kluwer/Plenum, New York.
- Heaton, N.J., Vold, R.L., and Vold, R.R. 1989. Deuterium quadrupole echo study of urea motion in urea/n-alkane inclusion compounds. *J. Am. Chem. Soc.* **111**: 3211–3217.
- Hodsdon, M.E. and Cistola, D.P. 1997. Ligand binding alters the backbone mobility of intestinal fatty acid-binding protein as monitored by ^{15}N NMR relaxation and ^1H exchange. *Biochemistry* **36**: 2278–2290.
- Hodsdon, M.E. and Frieden, C. 2001. Intestinal fatty acid binding protein: The folding mechanism as determined by NMR studies. *Biochemistry* **40**: 732–742.
- Hunston, D.L. and Klotz, I.M. 1971. Proton exchange in aqueous urea solutions. *J. Phys. Chem.* **75**: 2123–2127.
- Ishimura, M. and Uedaira, H. 1990. Natural-abundance oxygen-17 magnetic relaxation in aqueous solutions of apolar amino acids and glycine peptides. *Bull. Chem. Soc. Jpn.* **63**: 1–5.
- Jóhannesson, H., Denisov, V.P., and Halle, B. 1997. Dimethyl sulfoxide binding to globular proteins: A nuclear magnetic relaxation dispersion study. *Protein Sci.* **6**: 1756–1763.
- Kallies, B. 2002. Coupling of solvent and solute dynamics—molecular dynamics simulations of aqueous urea solutions with different intramolecular potentials. *Phys. Chem. Chem. Phys.* **4**: 86–95.
- Kauzmann, W. 1959. Some factors in the interpretation of protein denaturation. *Adv. Protein Chem.* **14**: 1–63.
- Kawahara, K. and Tanford, C. 1966. Viscosity and density of aqueous solutions of urea and guanidine hydrochloride. *J. Biol. Chem.* **241**: 3228–3232.
- Kelly, S.M. and Price, N.C. 1997. The application of circular dichroism to studies of protein folding and unfolding. *Biochim. Biophys. Acta* **1338**: 161–185.
- Kim, K. and Frieden, C. 1998. Turn scanning by site-directed mutagenesis: Application to the protein folding problem using the intestinal fatty acid binding protein. *Protein Sci.* **7**: 1821–1828.
- Kim, K., Ramanathan, R., and Frieden, C. 1997. Intestinal fatty acid binding protein: A specific residue in one turn appears to stabilize the native structure and be responsible for slow refolding. *Protein Sci.* **6**: 364–372.
- Klein-Seetharaman, J., Oikawa, M., Grimshaw, S.B., Wirmer, J., Duchardt, E., Ueda, T., Imoto, T., Smith, L.J., Dobson, C.M., and Schwalbe, H. 2002. Long-range interactions within a nonnative protein. *Science* **295**: 1719–1722.
- Koradi, R., Billeter, M., and Wüthrich, K. 1996. MOLMOL: A program for display and analysis of macromolecular structures. *J. Mol. Graph.* **14**: 51–55.
- Kuharski, R.A. and Rossky, P.J. 1984. Molecular dynamics study of solvation in urea–water solution. *J. Am. Chem. Soc.* **106**: 5786–5793.
- Kurian, E. 1998. “Solution structure of intestinal fatty acid binding protein complexed with 1-anilino-naphtalene-8-sulfonate: Implications for ligand binding.” Ph.D. thesis, Mayo Foundation, Rochester, MN.
- Liepinsh, E. and Otting, G. 1994. Specificity of urea binding to proteins. *J. Am. Chem. Soc.* **116**: 9670–9674.
- Likic, V.A. and Prendergast, F.G. 2001. Dynamics of internal waters in fatty acid binding protein: Computer simulations and comparison with experiments. *Proteins* **43**: 65–72.
- Likic, V.A., Juranic, N., Macura, S., and Prendergast, F.G. 2000. A “structural” water molecule in the family of fatty acid binding proteins. *Protein Sci.* **9**: 497–504.
- Lumb, K.J. and Dobson, C.M. 1992. ^1H nuclear magnetic resonance studies of the interaction of urea with hen lysozyme. *J. Mol. Biol.* **227**: 9–14.
- Miller, S., Janin, J., Lesk, A.M. and Chothia, C. 1987. Interior and surface of monomeric proteins. *J. Mol. Biol.* **196**: 641–656.
- Millet, I.S., Doniach, S., and Plaxco, K.W. 2002. Toward a taxonomy of the denatured state: Small angle scattering studies of unfolded proteins. *Adv. Protein Chem.* **62**: 241–262.
- Modig, K., Rademacher, M., Lücke, C., and Halle, B. 2003. Water dynamics in the large cavity of three lipid-binding proteins monitored by ^{17}O magnetic relaxation dispersion. *J. Mol. Biol.* **332**: 965–977.
- Myers, J.K., Pace, N.C., and Scholtz, J.M. 1995. Denaturant m values and heat capacity changes: Relation to changes in accessible surface areas of protein unfolding. *Protein Sci.* **4**: 2138–2148.
- Nicholls, A., Bharadwaj, R., and Honig, B. 1993. GRASP: Graphical representation and analysis of surface properties. *Biophys. J.* **64**: 166–170.
- Nikiforovich, G.V. and Frieden, C. 2002. The search for local native-like nucleation centers in the unfolded state of β -sheet proteins. *Proc. Natl. Acad. Sci.* **99**: 10388–10393.
- Pace, C.N. 1986. Determination and analysis of urea and guanidine hydrochloride denaturation curves. *Methods Enzymol.* **131**: 266–280.
- Pike, A.C.W. and Acharya, K.R. 1994. A structural basis for the interaction of urea with lysozyme. *Protein Sci.* **3**: 706–710.
- Press, W.H., Flannery, B.P., Teukolsky, S.A., and Vetterling, W.T. 1992. *Numerical recipes in C. The art of scientific computing*, 2nd ed. Cambridge University Press, Cambridge, UK.
- Ropson, I.J. and Dalessio, P.M. 1997. Fluorescence spectral changes during the folding of intestinal fatty acid binding protein. *Biochemistry* **36**: 8594–8601.
- Ropson, I.J. and Frieden, C. 1992. Dynamic NMR spectral analysis and protein folding: Identification of a highly populated folding intermediate of rat intestinal fatty acid-binding protein by ^{19}F NMR. *Proc. Natl. Acad. Sci.* **89**: 7222–7226.
- Ropson, I.J., Gordon, J.I., and Frieden, C. 1990. Folding of a predominantly β -structure protein: Rat intestinal fatty acid binding protein. *Biochemistry* **29**: 9591–9599.
- Santoro, M. and Bolen, D.W. 1998. Unfolding free energy changes determined by the Linear extrapolation method. I. Unfolding of phenylmethanesulfonyl α -chymotrypsin using different denaturants. *Biochemistry* **27**: 8063–8068.
- Scapin, G., Gordon, J.I., and Sacchettini, J.C. 1992. Refinement of the structure of recombinant rat intestinal fatty acid-binding apoprotein at 1.2-Å resolution. *J. Biol. Chem.* **267**: 4253–4269.
- Schellman, J.A. 1987. Selective binding and solvent denaturation. *Biopolymers* **26**: 549–559.
- . 1990. A simple model for solvation in mixed solvents. Application to the stabilization and destabilization of macromolecular structures. *Biophys. Chem.* **37**: 121–140.
- . 1994. The thermodynamics of solvent exchange. *Biopolymers* **34**: 1015–1026.
- Schellman, J.A. and Gassner, N.C. 1996. The enthalpy of transfer of unfolded proteins into solutions of urea and guanidinium chloride. *Biophys. Chem.* **59**: 259–275.
- Shimizu, S. and Chan, H.S. 2002. Origins of protein denatured state compactness and hydrophobic clustering in aqueous urea: Inferences from nonpolar potentials of mean force. *Proteins* **49**: 560–566.
- Shortle, D. 1996a. The denatured state (the other half of the folding equation) and its role in protein stability. *FASEB J.* **10**: 27–34.
- . 1996b. Structural analysis of non-native states of proteins by NMR methods. *Curr. Opin. Struct. Biol.* **6**: 24–30.
- Shortle, D. and Ackerman, M.S. 2001. Persistence of native-like topology in a denatured protein in 8 M urea. *Science* **293**: 487–489.
- Slichter, C.P. 1989. *Principles of magnetic resonance*, 3rd ed. Springer, Berlin.

- Sokolic, F., Idrissi, A., and Perera, A. 2002. Concentrated aqueous urea solutions: A molecular dynamics study of different models. *J. Chem. Phys.* **116**: 1636–1646.
- Stokes, R.H. 1967. Thermodynamics of aqueous urea solutions. *Aust. J. Chem.* **20**: 2087–2100.
- Tanford, C. 1970. Protein denaturation. Part C. Theoretical models for the mechanism of denaturation. *Adv. Protein Chem.* **24**: 1–95.
- Tirado-Rives, J., Orozco, M., and Jorgensen, W.L. 1997. Molecular dynamics simulations of the unfolding of barnase in water and 8 M aqueous urea. *Biochemistry* **36**: 7313–7329.
- Vanzi, F., Madan, B., and Sharp, K. 1998. Effect of the protein denaturants urea and guanidinium on water structure: A structural and thermodynamic study. *J. Am. Chem. Soc.* **120**: 10748–10753.
- Vold, R.L., Daniel, E.S., and Chan, S.O. 1970. Magnetic resonance measurements of proton exchange in aqueous urea. *J. Am. Chem. Soc.* **92**: 6771–6776.
- Wetlaufer, D.B., Malik, S.K., Stoller, L., and Coffin, R.L. 1964. Nonpolar group participation in the denaturation of proteins by urea and guanidinium salts. Model compound studies. *J. Am. Chem. Soc.* **86**: 508–514.
- Wiesner, S., Kurian, E., Prendergast, F.G., and Halle, B. 1999. Water molecules in the binding cavity of intestinal fatty acid binding protein: Dynamic characterization by water ^{17}O and ^2H magnetic relaxation dispersion. *J. Mol. Biol.* **286**: 233–246.
- Wu, J.-W. and Wang, Z.-X. 1999. New evidence for the denaturant binding model. *Protein Sci.* **8**: 2090–2097.
- Yeh, S.R., Ropson, I.J., and Rousseau, D.L. 2001. Hierarchical folding of intestinal fatty acid binding protein. *Biochemistry* **40**: 4205–4210.
- Yoshida, K., Ibuki, K., and Ueno, M. 1998. Pressure and temperature effects on ^2H spin-lattice relaxation times and ^1H chemical shifts in tert-butyl alcohol- and urea- D_2O solutions. *J. Chem. Phys.* **108**: 1360–1367.
- Zimmerman, A.W. and Veerkamp, J.H. 2002. New insights into the structure and function of fatty acid-binding proteins. *Cell. Mol. Life Sci.* **59**: 1096–1116.